Title: Proline Dehydrogenase-entrapped mesoporous magnetic silica nanomaterial for electrochemical biosensing of L-proline in biological fluids

Authors: Mohammad Hasanzadeh, Soodabeh Hassanpour, Arezoo Saadati Nahr, Nasrin Shadjou, Ahad Mokhtarzadeh, Jalal Mohammadi

PII: S0141-0229(17)30099-6
DOI: http://dx.doi.org/doi:10.1016/j.enzmictec.2017.05.007
Reference: EMT 9081

To appear in: *Enzyme and Microbial Technology*

Received date: 4-4-2017
Revised date: 26-5-2017
Accepted date: 27-5-2017

Please cite this article as: Hasanzadeh Mohammad, Hassanpour Soodabeh, Nahr Arezoo Saadati, Shadjou Nasrin, Mokhtarzadeh Ahad, Mohammadi Jalal.Proline Dehydrogenase-entrapped mesoporous magnetic silica nanomaterial for electrochemical biosensing of L-proline in biological fluids.*Enzyme and Microbial Technology* http://dx.doi.org/10.1016/j.enzmictec.2017.05.007

Proline Dehydrogenase-entrapped mesoporous magnetic silica nanomaterial for electrochemical biosensing of L-proline in biological fluids

Mohammad Hasanzadeh [a,*], Soodabeh Hassanpour [b], Arezoo Saadati Nahr [c], Nasrin Shadjou [d,e], Ahad Mokhtarzadeh [f,b], Jalal Mohammadi [b]

[a] Drug Applied Research Center, Tabriz University of Medical Sciences, Tabriz 51664, Iran.

[c] Pharmaceutical Analysis Research Center, Tabriz University of Medical Sciences, Tabriz, Iran.

[b] Department of Biochemistry, Higher Education Institute of Rab-Rashid, Tabriz, Iran.

[d] Department of Nanochemistry, Nano Technology Research Center, Urmia University, Urmia 57154, Iran.

[e] Department of Nano Technology, Faculty of Science, Urmia University, Urmia 57154, Iran.

[f] Immunology Research Center, Tabriz University of Medical Sciences, Tabriz, Iran.

Corresponding Author

E-mail address: (*) mhmmd_hasanzadeh@yahoo.com,hasanzadehm@tbzmed.ac.ir

Tel: +98(41) 33363311; Fax: +98(41)33363231

Highlights

- The immobilization of proline dehydrogenase on magnetic mesoporous silica nanomaterial was studied using electrochemical techniques.
- A thermostable biosensor for detection of L-proline was developed.
- The method was applied to assay L-proline in whole blood and cell lysates.

Abstract

In this work, physical adsorption was used for immobilization of proline dehydrogenase onto a magnetic mesoporous silica nanomaterial. The immobilization and electrocatalytical activity of proline dehydrogenase entrapped in a magnetic mesoporous silica nanomaterial was studied using cyclic voltammetry, differential pulse voltammetry, and square wave voltammetry. The magnetic mesoporous silica networks having a high surface area (362 $m^2 g^{-1}$) exhibited excellent properties for entrapment of proline dehydrogenase. The applied approach led to better resistance to temperature and pH inactivation in comparison to the free enzyme. The electrocatalytic current response of proline dehydrogenase entrapped in a magnetic mesoporous silica nanomaterial towards oxidation of L-proline was maintained in the analytical solution temperature up to 70 °C. The entrapped proline dehydrogenase was casted onto a polycysteine-modified glassy carbon electrode. The electrode was evaluated as an electrochemical biosensor for electrooxidation and determination of L-proline in phosphate buffer solution. A cyclic voltammetry study indicated that the oxidation process of proline is irreversible and is diffusion controlled. The electrochemical behavior was further exploited as a sensitive detection scheme for L-proline determination by differential-pulse voltammetry. Under optimized conditions, the concentration range and detection limit were 0.01-0.15 µM and 0.006 µM, respectively. The method was applied to the assay of L-proline in whole blood and normal and malignant cell line lysates ((normal cell (L929); gastric cancer cell-CAT 3, colon cancer cell-HCT, colon cancer cell-SW, and breast cancer cell-MCF7).

Keywords: Enzyme biosensing, proline dehydrogenase, mesoporous silica, magnetic nanoparticle, immobilization, signal amplification

1. Introduction

Proline dehydrogenase (PRODH), the first enzyme in the proline degradative pathway, plays a distinctive role in tumorigenesis and tumor development. PRODH possesses a variety of regulatory functions, such as redox homeostasis, osmotic adjustment, protection against metabolic stress, and providing signaling in a variety of organisms, including bacteria, plants, and mammals etc. [1-8]. As the only proteinogenic secondary amino acid, proline has special metabolic features [9, 10]. Not only does proline have its own family of enzymes, but also its catabolism, initiated by PRODH, is metabolically linked with several other core metabolic pathways in the human body. Therefore, detection and sensitive determination of this amino acid is often requested by clinicians. One of the best candidates for this purpose is enzyme-based biosensing and especially electrochemical enzymatic biosensors [11]. These types of sensor combine enzyme layers with electrochemical transducers to produce a biosensor and promise to provide a simple, accurate and inexpensive platform for patient diagnosis. Electrochemical methods are well suited to enzyme investigation [11]. Sensitive electrochemical-signaling strategies based on the direct or catalyzed oxidation of enzyme bases, and the redox reactions of reporter molecules or enzymes recruited to the electrode surface by specific enzyme probetarget interactions and charge-transport reactions mediated by the π-stacked base pairs have all been demonstrated [12].

In order to get successful enzyme-based biosensing strategy, enzymes must be immobilized onto suitable solid supports while preserve their biological activity [13]. This could also supply increasing the catalytic activity of enzyme towards harsh conditions. For example, the resistance to heat was attributed to the protective effect of the solid supports matrix, which prevents the protein undergoing extensive conformational changes inside the pores of a solid support. Despite the vast promise of extended stability and activity in harsh situations, enzyme-biosensing applications of silica-based mesoporous materials are rarely investigated.

4 In order to improve electron transfer and extend the life of enzyme biosensors, the use of nanomaterials as carriers/hosts to immobilize enzymes is promising [13].

Compared to polymers, an inorganic mesoporous material is an excellent support for molecular catalysts due to its strong chemical and thermal durability [14]. However, an extremely hydrothermally stable mesoporous material has not only all the virtues of an inorganic material but also has a large specific surface area, well-defined tunable pore sizes and an adjustable hydrophilic or hydrophobic nature, which provides enormous opportunities for immobilization of large catalytic species and catalytic conversion of bulky organic substrates [15-16]. Therefore, silica mesoporous materials are suitable candidates for hosting enzymes thanks to their unique advantages such as specific high surface area and large pore volume, and tunable/uniform pore size, as well as defined pore geometry, which could also supply fast transport of substrates and products to and from the biologically-active sites in the material [17-20].

In the present work, an electrochemical biosensor for detection of L-Pro was developed involving entrapment of PRODH onto Fe_3O_4-MCM-41-$nPrNH_2$ and its casting on PCys supported CS. Due to important property of silica mesoporous nanomaterials on enzyme biosensing and at continuing our study on the preparation and use of advanced nanomaterials for the electroanalytical determination of amino acids [21-37] in the present work, the preparation of a new electrochemical biosensor using PRODH loaded on Fe_3O_4-MCM-41-$nPrNH_2$ was described. The analytical performance of biosensor for quantification of L-Pro at physiological pH was investigated by DPV. To the best of our knowledge, in the case of amino acid sensing, silica mesoporous nanomaterials have been used for detection of tyrosine [38] using immobilization of tyrosinase on the surface of silica mesoporous materials and there was no further application for enzymatic biosensing of amino acids based on magnetic 5

mesoporous silica. This is the first report on determination of L-Pro using PRODH immobilized into Fe_3O_4-MCM-41-$nPrNH_2$.

2. Experimental

2.1. Reagent and chemicals

All chemicals used in this work were of analytical reagent grade, from Merck (Germany). The standard solution of L-Pro was prepared by dissolving an accurate mass of the bulk L-Pro in an appropriate volume of 0.1M phosphate buffer solution, pH 7.4 (PBS) (which was also used as the supporting electrolyte), and then stored in the dark at 4 ˚C. Additional dilute solutions were prepared daily by accurate dilution just before use. L-Pro solutions were stable and their concentrations did not change with time.

2.2. Apparatus

Electrochemical measurements were carried out in a conventional three-electrode cell (from Metrohm) powered by an electrochemical system comprising of AUTOLAB system with PGSTAT302N (Eco Chemie, Utrecht, The Netherlands). The system was run on a PC using NOVA 1.7 software. The ac voltage amplitude used was 10 mV and the equilibrium time was 5 s. An Ag/AgCl-Sat'd KCl (from Metrohm) and a platinum wire were used as reference and counter electrodes, respectively. The working electrode was GCE. For differential-pulse voltammetry (DPV) measurements, a pulse width of 25 mV, a pulse time of 50 ms, and a scan rate of 100 mVs-1 were employed.

2.2.Cell Culture

Human breast cancer cell line MCF-7, KAT III, mouse fibrosarcoma cell line WEHI-164, and mouse normal control cell line L929 were obtained from the Iranian National Cell Bank (Pasteur Institute, Tehran, Iran). Cells were maintained in a humidified water-jacked incubator with 5% CO_2 at 37 ◦C in RPMI-1640 supplemented with 10% (v/v) fetal bovine 6

serum(FBS), penicillin (100U/mL), and streptomycin (100 µg/mL) (all purchased from Sigma, Germany).

2.3. Loading of PRODH inside Fe_3O_4-MCM-41-nPrNH_2

At first, Mobile crystalline material 41 having NH_2 group and doped with magnetic (Fe_3O_4) nanoparticles [Fe_3O_4-MCM-41-nPrNH_2] was synthesized and characterized (See supporting Information) by methodology developed by our group previously [39]. At the next step, amine functionalized mesoporous silica was added to PRODH and stirred for 24 h at room temperature in 0.1M (pH 7.4). The supernatant was separated from solid materials by centrifugation at 6000 rpm for 10 min.

2.4. Layer-By-Layer (LBL) electropolymerization of L-Cys supported *CS* on the surface of GCE

For the preparation thin film of PCys-CS on the surface of GCE, 0.005g of L-Cys was added to 7 mL PBS (pH=7.4) and transferred to electrochemical cell. PCys, films were electrodeposited on the surface of GCE by cyclic voltammetry (CV) in the potential range from -1.0 to 1 V vs. Ag/AgCl at a scan rate of 100 mV.s $^{-1}$ for 10 cycles (Fig. 1A). The first positive scan, an oxidation peak at +0.53 V was observed, which is attributed to the oxidation of the Cys. In the subsequent reversal scan, one reduction peaks were observed at -0.7 V vs. Ag/AgCl, which may be attributed to the reduction of L-Cys. It has been confirmed that monomer containing NH can be electropolymerized at the surface of electrode to form a conducting film via covalent bond (C–N) between electrode and NH. L-Cys has one NH_2 groups and that can easily be oxidized to produce NH· Covalent bond (C–N) is then formed by the free radical reaction of NH with GCE surface with excellent stability. Therefore, the covalent bond (C–N) might be formed between carbon electrode and the amino group of proline. It is important to point out that during the high potential scan rate, the amino free

radical will easily form and the polymerization of the poly amino acid film could be formed on the surface of the GCE.

Chitosan (CS) has been increasingly used for preparation of sensors due to its attractive properties that comprise of high permeability, good adhesion, excellent film-forming ability, nontoxicity, cheapness and a resistance to chemical modification. It also makes possible the electron transfer after its swelling in the reaction mixture due to its hydrophilic nature [40, 41]. In addition, chitosan can also be used as a dispersant to form a stable composite with polymers (PCys-CS in this study) which can form a steady film on the surface of various substrates. Therefore, at the next step of electrode preparation, the three-electrode system was transferred into 0.1 M HCl containing 2 g/L CS, and 20 repetitive cycle in the potential range from -0.1 to 0.15 V vs. Ag/AgCl at a scan rate of 100 $mV.s^{-1}$ (Fig. 1B). Therefore, PCys-CS was prepared in this step. It is known that the electron withdrawing oxygen-containing groups on PCys are beneficial to the combination with CS from the electrostatic point of view, since CS dissolved in acid (HCl in the present work) is positively charged. Therefore, the hydrophilic CS can be interact PCys via -SH and $-NH_3^+$ side groups, which allow forming distinctive self-assembly network between the CS chains. Finally, thin film of PCys-CS was obtained at the surface of GCE.

2.5. Preparation of PRODH-Fe_3O_4-MCM-41-$nPrNH_2$ modified GCE

For preparation of enzyme biosensor, GCE electrode (2 mm in diameter) was polished to a mirror-like finish with 0.3 and 0.05 µm alumina slurry (Beuhler, USA) followed by rinsing thoroughly with double distilled water. Then it was successively sonicated in acetone and double distilled water, and allowed to dry at room temperature. Then, PRODH-MCM-41-$nPrNH_2$ was immobilized on Au surface and incubated for 24 h in 24 ˚C. Afterwards, the modified electrodes were rinsed with double distilled water. Finally, of PRODH-Fe_3O_4-MCM-41-$nPrNH_2$-GCE was obtained.

2.6. Immobilization of PRODH-Fe_3O_4-MCM-41-$nPrNH_2$ on PCys-*CS modified GC electrode*

In this step, PRODH-Fe_3O_4-MCM-41-$nPrNH_2$ was immobilized on the surface of GCE premodified by PCys- supported CS. Scheme 1, shows different modification steps.

2.7. Characterization different step of electrode modification

FEG-SEM images of GCE, PCys-GCE, PCys-CS-GCE, and PCys-CS-PRODH-Fe_3O_4-MCM-41-$nPrNH_2$-GCE are shown in Fig. 2. PCys electropolymerized directly on GCE, in the absence of CS as matrix, displays a regular dispersion. If the CS was coated on PCys-GCE, an irregular and spongy film can be observed. The following deposition of CS on the PCys-GCE providing an efficient interface for the following combination with Fe_3O_4- MCM-41-$nPrNH_2$ (Fig. 3). Finally, these results confirmed that the GCE was coated by PCysCS-PRODH-Fe_3O_4-MCM-41-$nPrNH_2$ film, leading to the change in the surface activity of the electrode. As mentioned above, the electron withdrawing oxygen-containing groups on PCys are beneficial to the combination with CS from the electrostatic point of view, since CS dissolved in acid (HCl in the present work) is positively charged. Therefore, CS can play a key role in the formation of a regular and high ordered polymeric film which was confirmed by FEG-SEM image of PCys-CS-GCE. On the one hand, SH-containing groups on PCys can provide large amounts of active sites for interaction with amine groups of CS and successful electrostatic interaction between PCys-CS (SH…NH). Therefore, the thiol-containing groups on PCys are also beneficial to the combination with CS from the electrostatic point of view. Consequently, PCys form long-range chemical bonding interactions with CS. Therefore, a biocompatible polymer (PCys-CS) with low toxicity can be fabricated on the surface of GCE. In general, scheme 1 shows the preparation steps of PCys-CS modified GC electrode.

3. Results and discussion

3.1. Comparison the performance of prepared electrodes

The electrochemical behaviour of L-Pro have been analyzed by measuring the CVs at different modified electrodes. Fig. 4 demonstrates a comparison of cyclic voltammograms (CVs) of 30mM L-Pro in phosphate buffer solution (0.1 M, pH=7.4) at the PRODH- Fe_2O_3-MCM-41-$nPrNH_2$-GCE, PRODH-Fe_2O_3-MCM-41-$nPrNH_2$-PCys-GCE, and PRODH- Fe_2O_3-MCM-41-$nPrNH_2$-PCys-CS-GCE. As can be seen, no response at the surface of bare GCE is observed at 1.49V. In Fig.4 A-C it was demonstrated that the anodic peak current response increases noticeably at the PRODH-MMSNP-$nPrNH_2$-GCE which shows the significant role of Fe_2O_3-MCM-41-$nPrNH_2$. The CV of PRODH- Fe_2O_3-MCM-41-$nPrNH_2$-PCys-GCE exhibited higher current than PRODH- Fe_2O_3-MCM-41-$nPrNH_2$-GCE, which shows that Fe_2O_3-MCM-41-$nPrNH_2$-PCys composite film has a large effective surface area than MMSNP-$nPrNH_2$. Furthermore, change of the resultant electrode with CS enhances the response of the electrode about 1.42 and 3.04 times on that obtained with the PRODH-Fe_2O_3-MCM-41-$nPrNH_2$-PCys-GCE and PRODH-Fe_2O_3-MCM-41-$nPrNH_2$-GCE, respectively, which can be related to the increased active surface area of the modified electrode and accumulation of L-Pro on the surface of the modified electrode. These results show the anodic peak current at the surface of PCys-CS-Fe_2O_3-MCM-41-$nPrNH_2$- GCE is significantly enhanced than PCys-GCE, PPR-CS-GCE while the cathodic peak current was decreased considerably. These results indicate that PCys-CS-Fe_2O_3-MCM-41- $nPrNH_2$-CS could accelerate the rate of electron transfer of L-Pro and have good electrocatalytic behaviour for redox reaction of L-Pro, which demonstrated that the nano-coatings of polymers deposited on the mesopore walls lead to a remarkably enhanced oxidation rates of L-Pro.

It is important to point out that, the amino group of L-Cys could enable PCys to be related??? with negatively charged groups of L-Pro through electrostatic interaction. Also, mesoporous silica with good geometric surface area, prepare a suitable substrate for dense loading of LPro in the presence of CS. It is no doubt that when CS and L-Cys were electro-polymerized at 10

the surface of GCE, the response current for L-Pro was greatly enhanced. In addition, the increasing oxidation peak and decreasing overvoltage of L-Pro confirm that Enzyme-PCysCS-Fe_2O_3-MCM-41-n$PrNH_2$- films have a high catalytic ability for oxidation of these analytes. Therefore, Enzyme-PCys-CS-Fe_2O_3-MCM-41-n$PrNH_2$ is suitable as a mediator to transfer electrons between L-Pro and the working electrode and enhance electrochemical regeneration following electron exchange with these analytes. Finally, as a decisive electrical component in the biopolymer film, PCys-Fe_2O_3-MCM-41-n$PrNH_2$-CS provides an enhancement for sensitive detection of L-Pro, meanwhile; PCys can amplify the electrochemical signals produced during the electrochemical sensing process. In summary, the synergistic effect of Fe_2O_3-MCM-41-n$PrNH_2$, PCys, and CS leads to a successful electrooxidation of L-Prol.

The electrocatalytic effect of the Enzyme-MCM-41-n$PrNH_2$-Au electrode can be ascribed to the combination of the electron-acceptor ability of NH_2 and confinement effects due to the attachment to the MCM-41 matrix. On the basis of the previous considerations, the electrocatalytic effect of Enzyme-MCM-41-n$PrNH_2$ modified electrode must result from the superposition of the effect associated with more external NH_2 units and that due to boundary-associated ones. On the other hand, since the catalytic effect associated with Enzyme-MCM-41-n$PrNH_2$ consists essentially of an enhancement of the anodic peak for Pro oxidation, the catalytic effect can tentatively be associated with a redox reaction in solution phase between NH_2 units and any intermediate species resulting from the initial electron transfer of L-Pro.

3.2. Biosensor selectivity

One of the most important problems to solve in the practical application of the prepared sensors is to minimize the effect of interfering species that may be present in real samples together with the analyte. Possible compounds that may interfere in the voltammetric determination of proline, such as uric acid (UA), ascorbic acid (AA), Glucose (AA), Tyrosine

(Tyr), Ascorbic acid (AA), Phenylalanine (Phe), Glycine (Gly), Serine (Ser), D-Alanine (D-Ala), L-Alanine (L-Ala), Arginine (Arg), Aspartic acid (Asp), Histidine (His), Cysteine (Cys), and Leucine (Leu), were investigated. CV measurements of the L-Pro and its mixture with different interfering species are shown in Fig. 5. As can be seen, none of these compounds oxidises or reduces at oxidation potential of L-Pro (E_{pa}=1.429), and it was confirmed that they have no interference in L-Pro determination. However, the peak currents were decreased witht he results shown in Fig. 5.3.

3.3. The effect of temperature on electrode stability

Fig. 6 shows the plots of the current response of 40 mM L-Pro at various temperatures of the PBS solution. Also, Fig. 5 shows dependence of the current response of L-Pro with a PRODH-Fe_2O_3-MCM-41-n$PrNH_2$-PCys-CS-GCE on the various temperature of PBS (0.1 M). As can be seen in Fig. 5, the current response was not changed with increase of the measurement temperature up to 313.15 °C. The applied approach led to better resistance temperature and pH inactivation in comparison to the free enzyme. The electrocatalytic current response of proline dehydrogenase entrapped magnetic mesoporous silica nanomaterial towards oxidation of L-Pro was maintained in the analytical solution temperature up to 313.15 °C.

3.4. Effect of scan rate

Scan rate is one of important items affecting electroactivity of various organic molecules. The electrooxidation of L-PRO at various scan rates was investigated on the surface of PRODH-MMSNP-n$PrNH_2$-PCys-CS-GCE by CV technique. Thus, the effect of the scan rate on L-Pro electrooxidation was studied in the range from 20-200 mVs^{-1} using CV method (Fig. 12 7A). A linear relationship was achieved between the peak current and the scan rate in the range of 20-200 mVs^{-1}, which revealed that the oxidation of L-PRO was an adsorption-controlled step. Two approaches widely used to study the reversibility of reactions and to determine whether

a reaction is adsorption or diffusion controlled; Consist of the analyses of dependencies: Ip *vs* $v^{1/2}$ and ln I_p *vs* ln v. Fig. 7B shows these plots for the oxidation peak of L-PRO in 0.1M PBS. For reversible or irreversible systems without kinetic complications, I_{pa} varies linearly with $v^{1/2}$, intercepting the origin. Although, the plot of I_{pa} on $v^{1/2}$ presented in Fig. 7B is linear (R^2 =0.9914), it crosses the origin of the axes. In the scan rate range from 60-350 mVs^{-1}, oxidation peak current (I_p) of L-Pro electrooxidation depends linearly on the square root of the scan rate (v) and is described by the following equation:

I_{pa} (A) = 34.903 $v^{0.5}$ $(V.s^{-1})^{0.5}$ + 0.9655A (R^2 = 0.9914)

This dependence does not cross the origin (Fig. 7B). This fact can suggest that the electrode process of L-PRO electrooxidation isn't controlled by diffusion and can be preceded by chemical reaction. On the other hand, a dependence of ln I_{pa} on ln v is linear and described by the following equation:

ln I_{pa} =0.5157 ln v $(V\ s^{-1})$+9.0538 mA (R^2 = 0.9925)

Its slope is 0.5157 and indicates diffusion-control of the electrode process. A slope close to 0.5 is expected for diffusion-controlled electrode processes and close to 1.0 for adsorption-controlled processes [42, 43].

Fig. 7C presents a dependence of E_{pa} on scan rate determined from cyclic voltammograms recorded for the L-PRO electrooxidation. If electrochemical reaction is irreversible, then E_{pa} is independent on v. Thus, it can be concluded that heterogeneous electron transfer in L-PRO electrooxidation is irreversible because E_{pa} increases with an increase in the scan rate. In addition, the value of the overall electron transfer coefficient for the reaction can be obtained from the following equation [42, 43].

$$Ep = \left(\frac{RT}{2\alpha F}\right) \ln v + constant \qquad (1)$$

Where E_p-peak potential (V), R-universal gas constant (8.314 J K^{-1} mol^{-1}), F-Faraday constant (96,487 C mol^{-1}), T-Kelvin temperature (298 K), α -anodic transfer coefficient, *v*-scan rate (V. s^{-1}).

Using the relation of anodic peak potential on the logarithm of the scan rate (Fig. 7C), the value of the overall electron transfer coefficient (β_n) was obtained as 0.521 for L-PRO electrooxidation.

3.5. Analytical Approach

As a highly sensitive electrochemical method, the DPV has much higher current sensitivity and better resolution compared to CV. Therefore, DPV method is used for determination of L-Pro with the PRODH-Fe_3O_4-MCM-41-n$PrNH_2$-PCys-CS-GCE (Fig.8 A). Under the optimum conditions, with the increase of L-Pro concentrations, the DPV oxidation peaks increased gradually in standard samples (Fig. 8B&C). The results demonstrated that anodic peak current were proportional to L-Pro concentration intervals. The experimental conditions influencing the determination of L-Pro were optimized and under physiological pH, the oxidation peak current was proportional to L-Pro concentration in the range of 0.01-0.15 µM, while the low limit of quantification (LLOQ) was 0.006 µM.

3.6. Real sample analysis

According to the obtained results, it was possible to apply this technique to the quantitative analysis of L-Pro in real samples. As mentioned previously, the PBS of pH 7.4 was selected as the supporting electrolyte for the quantification of L-Pro. The linear range for the determination of L-Pro in whole blood was investigated under optimal conditions. Using DPV technique (Fig 9), the linear range for unprocessed whole blood without any pre-treatment was 1 µm to 10 nM. In addition, the LLOQ was 10 nM.

The analytical recoveries of added L-Pro from blood were determined in triplicate at concentrations of 1µM, 4 µM, and 50 mM. The respective mean values (all %) obtained were 100-110 (Table 2).

In addition, square wave voltammetry (SWV) technique was used for the analysis of L-Pro in different cancer cell culture media. To this end, using the developed biosensor and standard addition method, we analyzed for the detection of the L-Pro in normal cell (L929) and various cancer cell lines such as gastric cancer cell- CAT 3, colon cancer cell-HCT, colon cancer cell-SW, and breast cancer cell-MCF7. The engineered biosensor (PRODH-Fe_3O_4-MCM-41-n$PrNH_2$-PCys-CS-GCE) could detect the L-Pro in these samples. Fig. 10 and Table 3 shows the SWVs of L-Pro in the supernatants of the normal and various cancer cell lines cultured during three days. The application of the engineered biosensor showed that colon cancer cell-SW and breast cancer cell-MCF7 has lower and higher peak currents, respectively. These results confirmed application of engineered biosensor for diagnostic of cancer type and relationship of L-Pro with the investigated cancer cells.

4. Conclusions

In summary, an electrochemical biosensor for sensitive detection of L-Pro were developed involving PRODH,Fe_3O_4-MCM-41-n$PrNH_2$, PCys, and CS. Physical adsorption, the simplest approach has been used to immobilize PRODH onto Fe_3O_4-MCM-41-n$PrNH_2$. The method is simple to perform, non-destructive which are appropriate for preserving the biological activity of enzyme. The electrocatalytical behavior of PRODH-Fe_3O_4-MCM-41-n$PrNH_2$ immobilized on glassy carbon electrode was evaluated using cyclic voltammetry. The MMSN networks with high surface area (362 m^2 g^{-1}) exhibited excellent properties for entrapment of PRODH. The prepared electrode (PRODH-Fe_3O_4-MCM-41-n$PrNH_2$-PCys-CS) has higher current densities for the oxidation of L-Pro than PRODH-Fe_3O_4-MCM-41-n$PrNH_2$-PCys, PRODH-Fe_3O_4-MCM-41-n$PrNH_2$-GCE, and PRODH-GCE. These results indicated the

synergetic effect of PCys-CS and PRODH-Fe_3O_4-MCM-41-$nPrNH_2$ on the electrocatalytical oxidation of L-Pro. The electrocatalytic current response of PRODH-Fe_3O_4-MCM-41-$nPrNH_2$-PCys towards oxidation of L-Pro was maintained in the analytical solution temperature up to 70 °C. Also, it's found that, the combination of mesoporous silica with conducting/redox polymers is favorable, since mesoporous silica can increase the electrical conductivity and mechanical strength of the resulting polymer-mesoporous silica hybrids, apart from the possibility of presenting superior analytical performances due to synergistic effects. Finally, this biosensor can be used as a voltammetric detector for routine analysis of L-Pro in flow systems when coupled to chromatographic and electrophoretic separation systems.

Acknowledgements

We gratefully acknowledge the financial support by the Ministry of Health and Medical Education of Iran (The Grant for Young assistant Professors), Tabriz University of Medical Sciences, for financial and instrumental supporting of this research.

5. References

1. Phang, J. M., Downing, S. J., Yeh, G. C., Smith, R. J., Williams, J. A., (1982) Stimulation of the hexosemonophosphate-pentose pathway by pyrroline-5-carboxylate in cultured cells. J. Cell Physiol. 110, 255-261.

2.Yeh, G. C., Roth, E. F. Jr., Phang, J. M., Harris, S. C., Nagel, R. L., (1984) The effect of pyrroline-5-carboxylic acid on nucleotide metabolism in erythrocytes from normal and glucose-6-phosphate dehydrogen ase-deficient subjects. J. Biol. Chem. 259, 5454–5458.

3. Phang, J. M. (1985) The regulatory functions of proline and pyrroline-5- carboxylic acid. Curr. Top. Cell Regul. 25, 91–132.

4. Peng, Z., Lu, Q., and Verma, D. P. (1996) Reciprocal regulation of delta1-pyrroline-5-carboxylate synthetase and proline dehydrogenase genes controls proline levels during and after osmotic stress in plants. Mol. Gen. Genet. 253, 334–341.

5. Schafer, I. A., Scriver, C. R., and Efron, M. L. (1962) Familial hyperprolinemia, cerebral dysfunction and renal anomalies occuring in a family with hereditary nephropathy and deafness. N. Engl. J. Med. 267, 51–60.

6. Phang, J. M., Hu, C. A., and Valle, D. (2001) Disorders of proline and hydroxyproline metabolism. In Metabolic and Molecular Bases of Inher ited Disease. (Scriver, C. R., Beaudet, A. L., Sly, W. S., Valle, D., eds.). pp. 1821–1838, McGraw-Hill, New York.

7. Bender, H. U., Almashanu, S., Steel, G., Hu, C. A., Lin, W. W., (2005) Functional consequences of PRODH missense mutations. Am. J. Hum. Genet. 76, 409–420.

8. Willis, A., Bender, H. U., Steel, G., and Valle, D. (2008) PRODH variants and risk for schizophrenia. Amino Acids 35, 673-679.

9. Phang, J. M., Liu, W., and Zabirnyk, O. (2010) Proline metabolism and microenvironmental stress. Annu. Rev. Nutr. 30, 441-463.

10. Phang, J. M. and Liu, W. (2012) Proline metabolism and cancer. Front Biosci. 17, 1835-1845.

11. H, Yang, Enzyme-based ultrasensitive electrochemical biosensors, (2012) Current Opinion in Chemical Biology 16, 422-428

12. R.K. Kobos, Enzyme-based electrochemical biosensors, Trends in Analytical Chemistry 6, 1987, 6-9.

13. Younes Jomma, Ezzaldeen; Ding, Shou-Nian. Recent Advances on Electrochemical Enzyme Biosensors, Current Analytical Chemistry, 12, 2016, 5-21

14. Naik, Bhanudas; Ghosh, Narendra N. A Review on Chemical Methodologies for Preparation of Mesoporous Silica and Alumina Based Materials. Recent Patents on Nanotechnology, Volume 3, Number 3, November 2009, pp. 213-224(12)

15. Sayari, A. Hamoudi, S. Periodic Mesoporous Silica-Based Organic−Inorganic Nanocomposite Materials. Chem. Mater. 13 (2001) 3151

16. Hasanzadeh M., Shadjou N., Eskandani M., de la Guardia M., Mesoporous silica-based materials for use in electrochemical enzyme nanobiosensors, Trends Analytical Chemistry, 40, 2012, 106

17. Walcarius A (1998) Analytical Applications of Silica-Modified Electrodes -A Comprehensive Review. Electroanalysis 10:1217–1235

18. Walcarius A (2001) Electrochemical Applications of Silica-Based Organic-Inorganic Hybrid Materials. Chem Mater 13: 3351-3372

19. Walcarius A (2001) Electroanalysis with Pure, Chemically Modified and Sol-Gel-Derived Silica-Based Materials. Electroanalysis 13: 701-718

20. Walcarius A (2013) Mesoporous materials and electrochemistry. Chem Soc Rev 42: 4098-4140.

21. Hasanzadeh M., Sadeghi S., Bageri L., Mokhtarzadeh A., Karimzadeh A., Shadjou N., Mahboob S., 2016. Poly-dopamine-beta-cyclodextrin: A novel nanobiopolymer towards sensing of some amino acids at physiological pH. Mater Sci Eng C 69:343-57.

22. Hasanzadeh M., Karimzadeh A., Shadjou N., Mokhtarzadeh A., Bageri L., Sadeghi S., Mahboob S. 2016. Graphene quantum dots decorated with magnetic nanoparticles: Synthesis, electrodeposition, characterization and application as an electrochemical sensor towards determination of some amino acids at physiological pH. Mater Sci Eng C 68:814-30 .

23. Shadjou, N., Hasanzadeh, M., Talebi, F., poursattar, A. 2016. Graphene quantum dot functionalized by beta-cyclodextrin: a novel nanocomposite toward amplification of l-cysteine electro-oxidation signals, Nanocomposites, 2, 18-28

24. Omidinia, E., Shadjou, N., Hasanzadeh, M., 2014. Immobilization of phenylalanine-dehydrogenase on nano-sized polytaurine: A new platform for application of nano-polymeric materials on enzymatic biosensing technology. Mater Sci Eng C 42, 368-373.

25. Omidinia, E., Shadjou, N., Hasanzadeh, M., 2014. Electrochemical nanobiosensing of phenylalanine using phenylalanine dehydrogenase incorporated on amino-functionalized mobile crystalline material-41. IEEE Sensor J. 14, 1081-1088 .

26. Omidinia E., Shadjou N, Hasanzadeh M., 2014. Aptamer-based Biosensor for Detection of Phenylalanine at Physiological pH. Appl Biochem Biotechnol. 172, 2070-80.

27. Omidinia E, Shadjou N, Hasanzadeh M., 2013. (Fe_3O_4)-graphene oxide as a novel magnetic nanomaterial for non-enzymatic determination of phenylalanine. Mater Sci Eng C 33, 4624-4632 .

28. Hasanzadeh, M., Shadjou, N., Omidinia, E., 2013. Mesoporous silica (MCM-41)-Fe_2O_3 as a novel magnetic nanosensor for determination of trace amounts of amino acids. Colloids Surf. B: Biointerfaces 108, 52-59

29. Saghatforoush L.A., Hasanzadeh M., Shadjou N. Polystyrene–graphene oxide modified glassy carbon electrode as a new class of polymeric nanosensors for electrochemical determination of histamine. Chin. Chem. Lett. 2014, 25, 655-658

30. Omidinia E., Khanehzar A., Shadjou N., Shahbaz Mohamadi H., Hojati Emami S., Hasanzadeh M. Covalent immobilization of phenylalanine dehydrogenase on glutaraldehyde modified poly (3, 4-ethylenedioxy) thiophene: poly (styrenesulfonate)/polyvinyl alcohol conducting polymer composite films for electrochemical detection of L-phenylalanine. Anal. Bioanal. Electrochem. 5, 2013, 597- 608

31. Hasanzadeh M., Shadjou N., Eskandani M., de la Guardia M, Mesoporous silica-based materials for use in electrochemical enzyme nanobiosensors, Trends Anal. Chem. 40, 2012, 106-118

32. Hasanzadeh M., Shadjou N., Chenc S.-T.,Sheikhzadeh P., MCM-41-NH_2 as an advanced nanocatalyst for electrooxidation and determination of amino acids. Catal. Commun. 19, 2012, 21-27

33. Saghatforoush L.A., Hasanzadeh M., Shadjou N., Hasanzadeh M., Khalilzadeh B., Deposition of new thia-containing Schiff-base iron (III) complexes onto carbon nanotube modified glassy carbon electrodes as a biosensor for electrooxidation and determination of amino acids. Electrochim. Acta. 56, 2011, 1051-1061

34. Hasanzadeh M., Karim-Nezhad G., Shadjou N., Hajjizadeh M., Khalilzadeh B., Saghatforoush L., Abnosi MH., Babaei A., Ershad S., 2009. Cobalt hydroxide nanoparticles modified glassy carbon electrode as a biosensor for electrooxidation and determination of some amino acids. Anal Biochem. 389,130-137 .

35. Khalilzadeh B., Hasanzadeh M., Bakhoday B., Babaei A., Hajjizadeh M., Zendehdel M., 2009. Zeolite nanoparticles-modified carbon paste electrode as a biosensor for simultaneous determination of Tryptophan and dopamine, J. Chin Chem Soc., 56, 789-796

36. Hasanzadeh M., Shadjou N., de la Guardia M, Eskandani M., 2012. Mesoporous silica-based materials for use in biosensors, Trends Anal. Chem. 33, 117-129

37. Massomi B.A., Fathalipour S., Massudi, A., Hasanzadeh M., Entezami, A.A. 2013. Ag/Polyaniline Nanocomposites: Synthesize, Characterization, and Application to the Detection of Dopamine and Tyrosine. J .Appl. Polymer Sci. 130, 4, 2780-2789

38. Wu S., Wang H., Tao S., Wang C., Zhang L., Liu Z., Meng C. 2011 Magnetic loading of tyrosinase-Fe3O4/mesoporous silica core/shell microspheres for high sensitive electrochemical biosensing, Anal. Chim. Acta, 686, 81-86

39. Hasanzadeh M, Pournaghi-Azar MH, Shadjou N, Jouyban A. Magnetic nanoparticles incorporated on functionalized mesoporous silica: an advanced electrochemical sensor for simultaneous determination of amiodarone and atenolol. RSC Advances. 2014;4, 4710-7.

40. Ling S.J. Yuan R. Chai Y.Q. Zhang T.T. Study on immunosensor based on gold nano-particles/chitosan and MnO_2 nanoparticles composites membrane/Prussian blue modified gold electrode, Bioprocess Biosyst. Eng. 32 (2009) 407-414.

41. Batra B. Pundir C.S. An amperometric glutamate biosensor based on immobilization of glutamate oxidase onto carboxylated multiwalled carbon nanotubes/gold nano-particles/chitosan composite film modified Au electrode, Biosens. Bioelectron. 47(2013) 496-501.

42 Kissinger P, Heineman WR (1996) Laboratory Techniques in Electroanal. Chem, Second Ed., CRC Press, New York, p. 224.

43. Bard AJ, Faulkner LR (2001) Electrochemical Methods: Fundamentals and Applications second ed., 236, John Wiley & Sons, New York, p. 503.

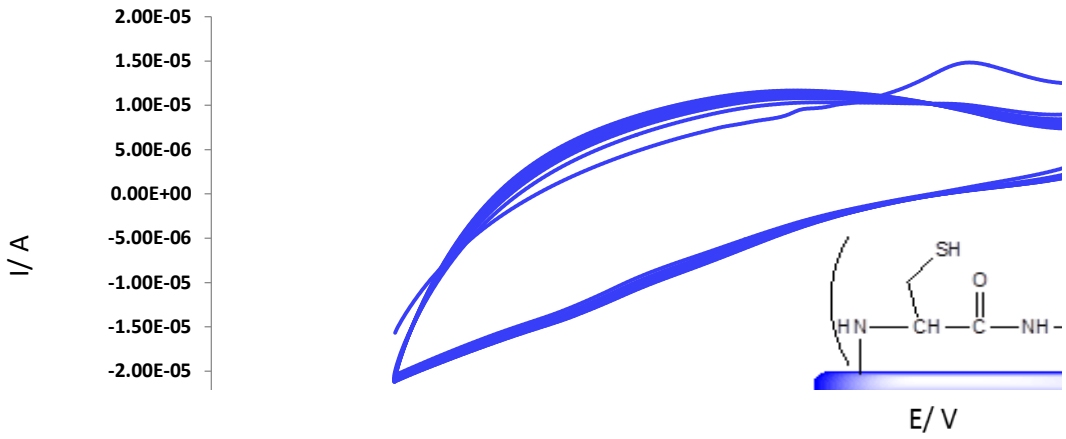

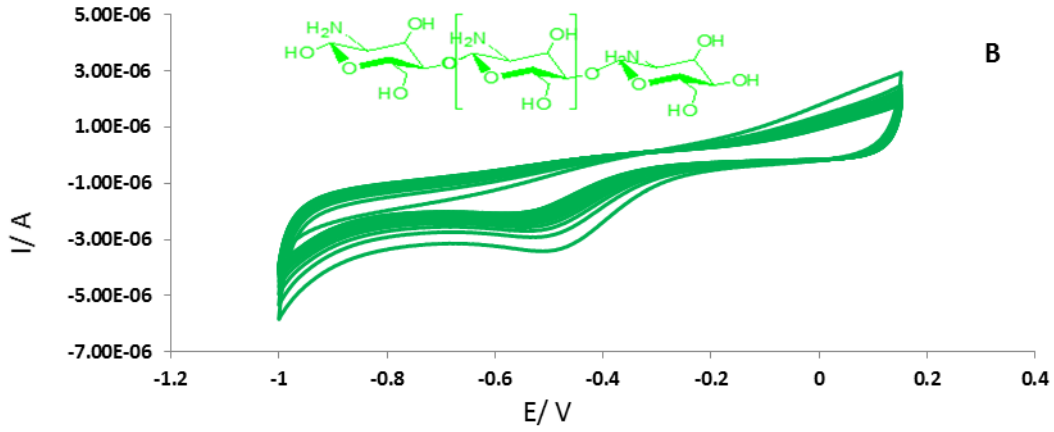

Fig.1. A) Electropolymerization of 0.005g L-Cys containing 0.1M PBS (pH=7.4) on the surface of GCE. Range of potential is -1.0 to +1.0 V with the scan rate of 100 $mV.s^{-1}$. Number of cycles=10. **B**) Electropolymerization of CS on the surface of PCys-GCE using repetitive CV. The solution was 0.1 M HCl containing 2 g/L CS. Number of cycles were 20 in the potential range from -0.1 to +0.15 V *vs.* Ag/AgCl at a scan rate of 100 mV/s

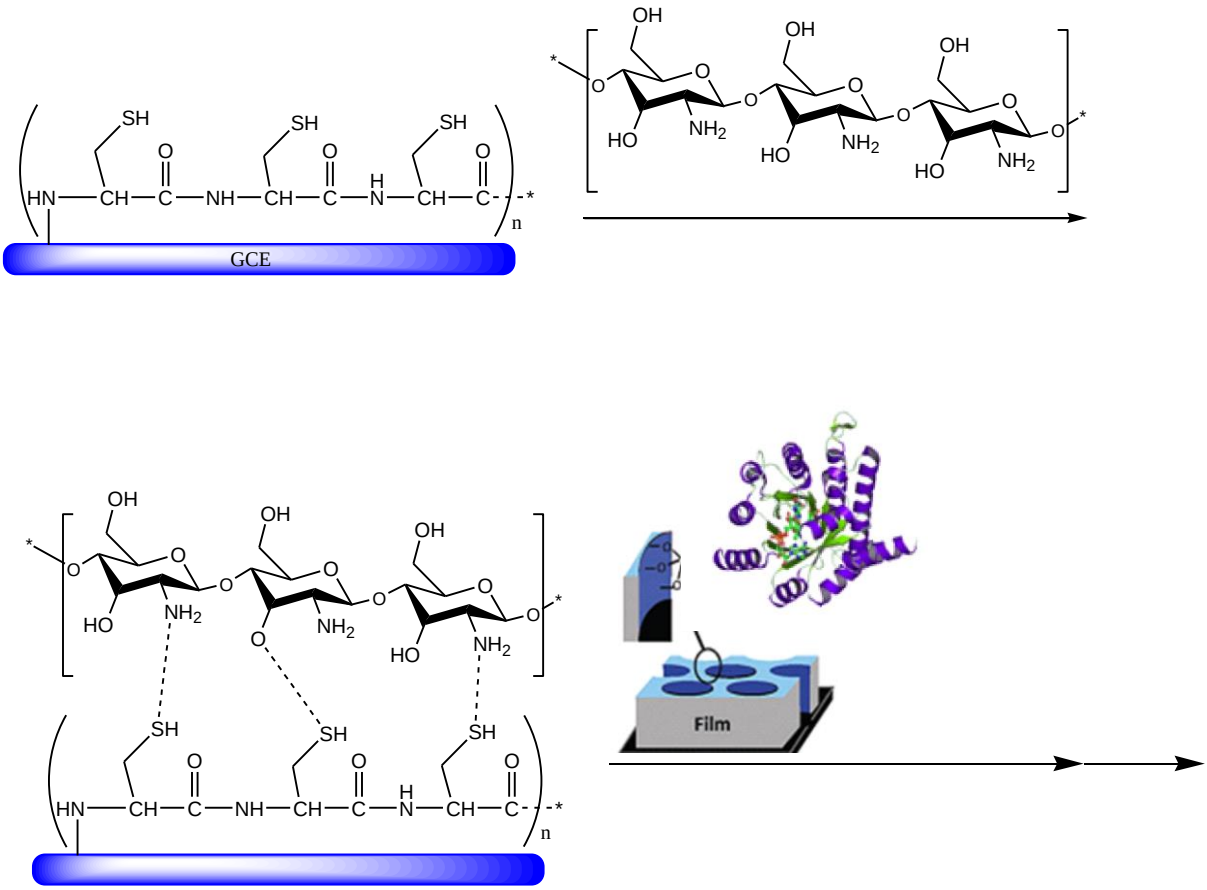

Scheme 1: Biosensor preparation procedure

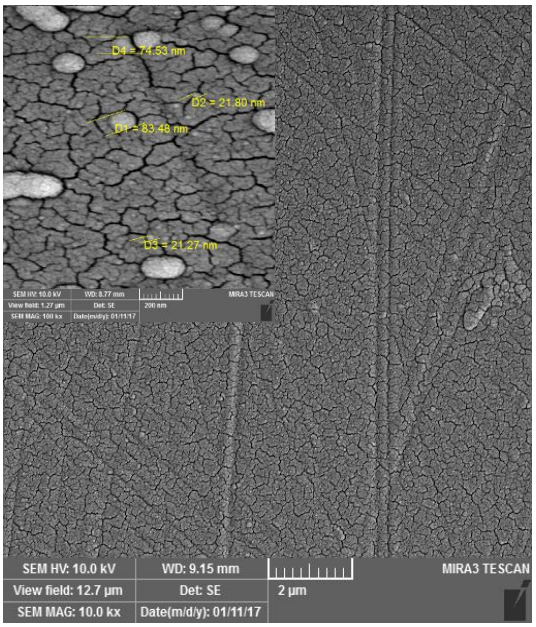

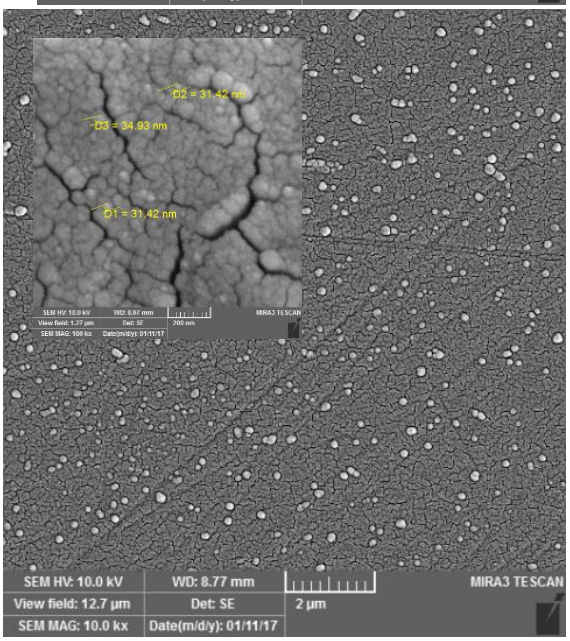

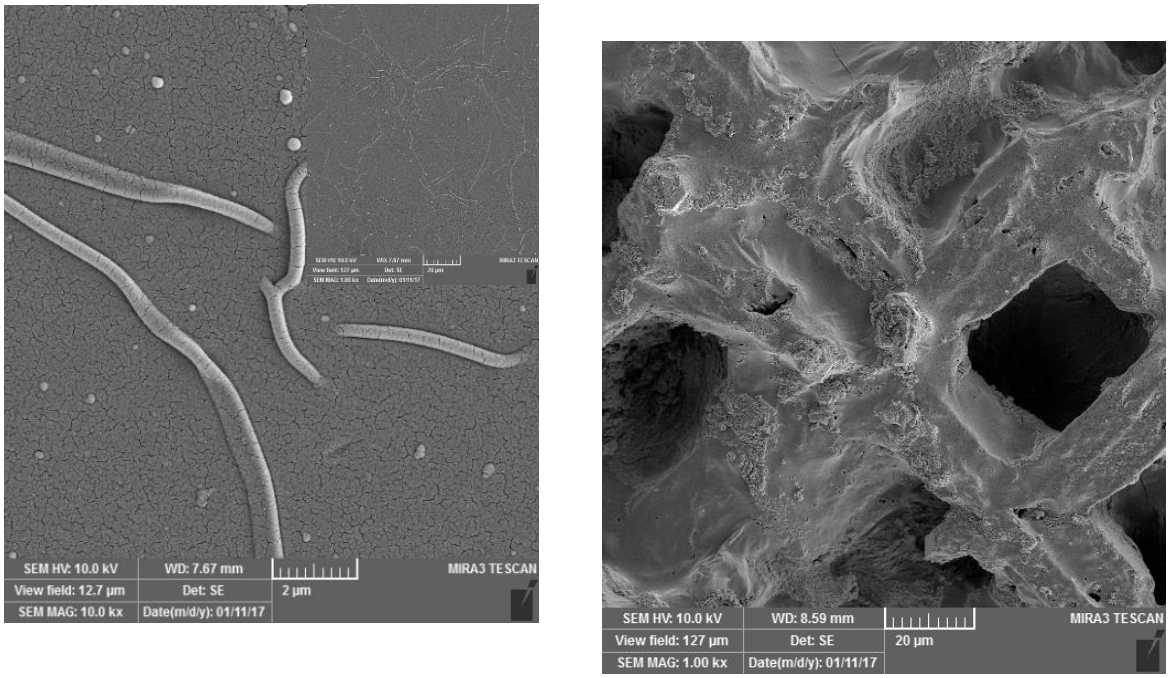

Fig. 2: FEG-SEM images of bare GCE, PCys-GCE, PCys-CS-GCE, and PRODH-MMSNP-n$PrNH_2$-PCys-CS-GCE in similar magnitude.

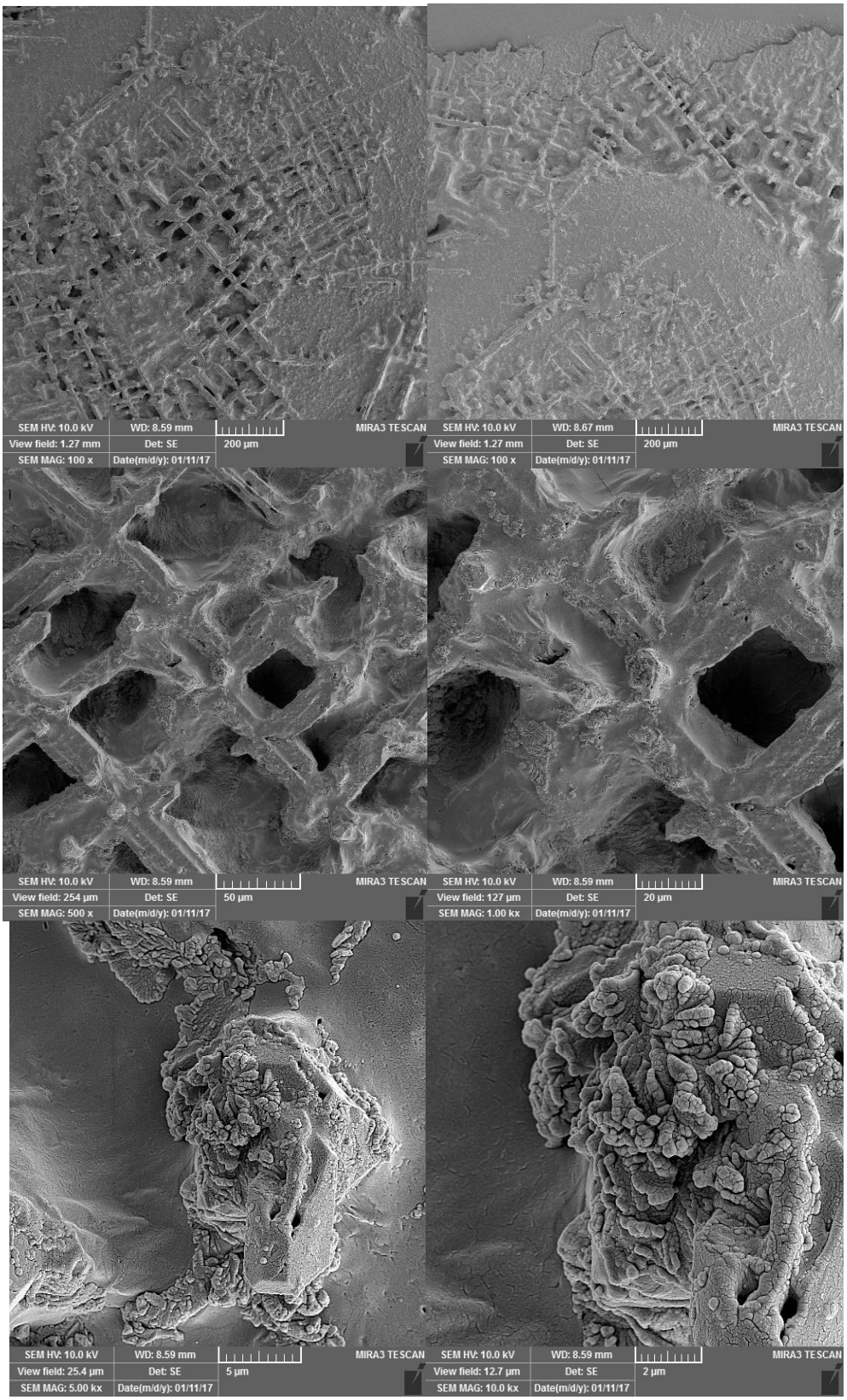

Fig. 3: FE-SEM images of PRODH-MMSNP-nPrNH$_2$-PCys-CS-GCE in different magnification

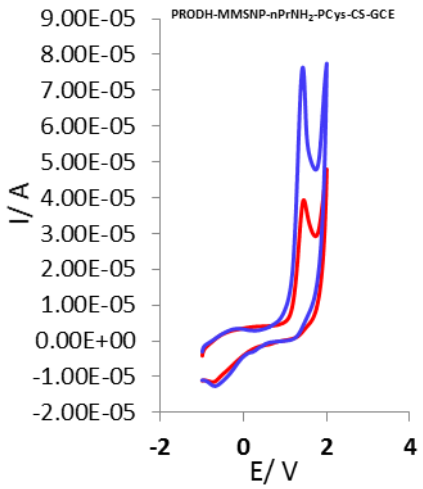

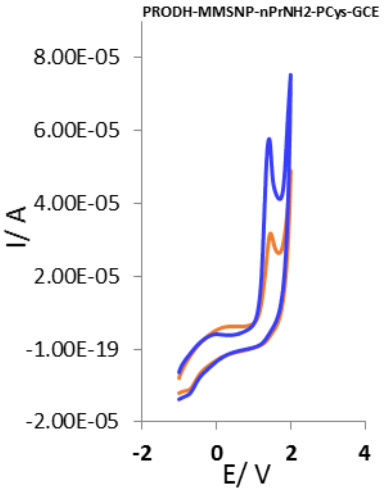

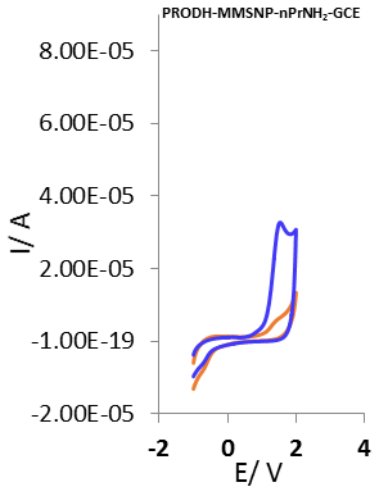

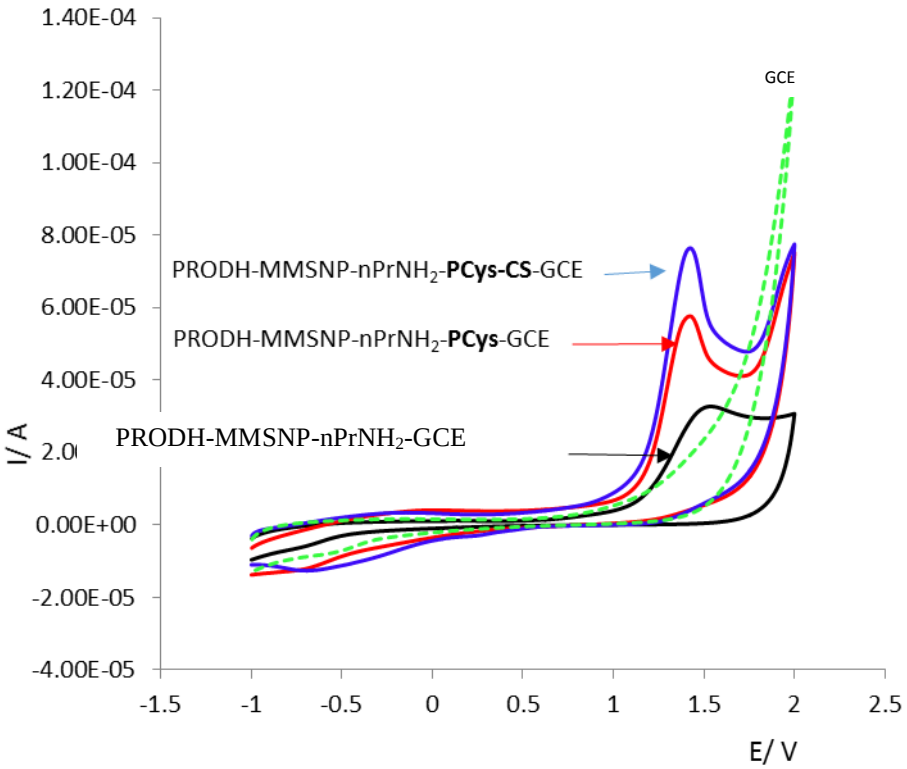

Fig. 4. (A-C) The CVs of PRODH-MMSNP-nPrNH$_2$-GCE, PRODH-MMSNP-nPrNH$_2$-PCys-GCE and PRODH-MMSNP-nPrNH$_2$-PCys-CS-GCE in PBS 0.1 M, pH= 7.4 at scan rate =100 mV s^{-1} in the absence (red) and presence (blue) of 34 mM of L-Pro. **D)** The over layer of different electrodes in the presence of L-Pro

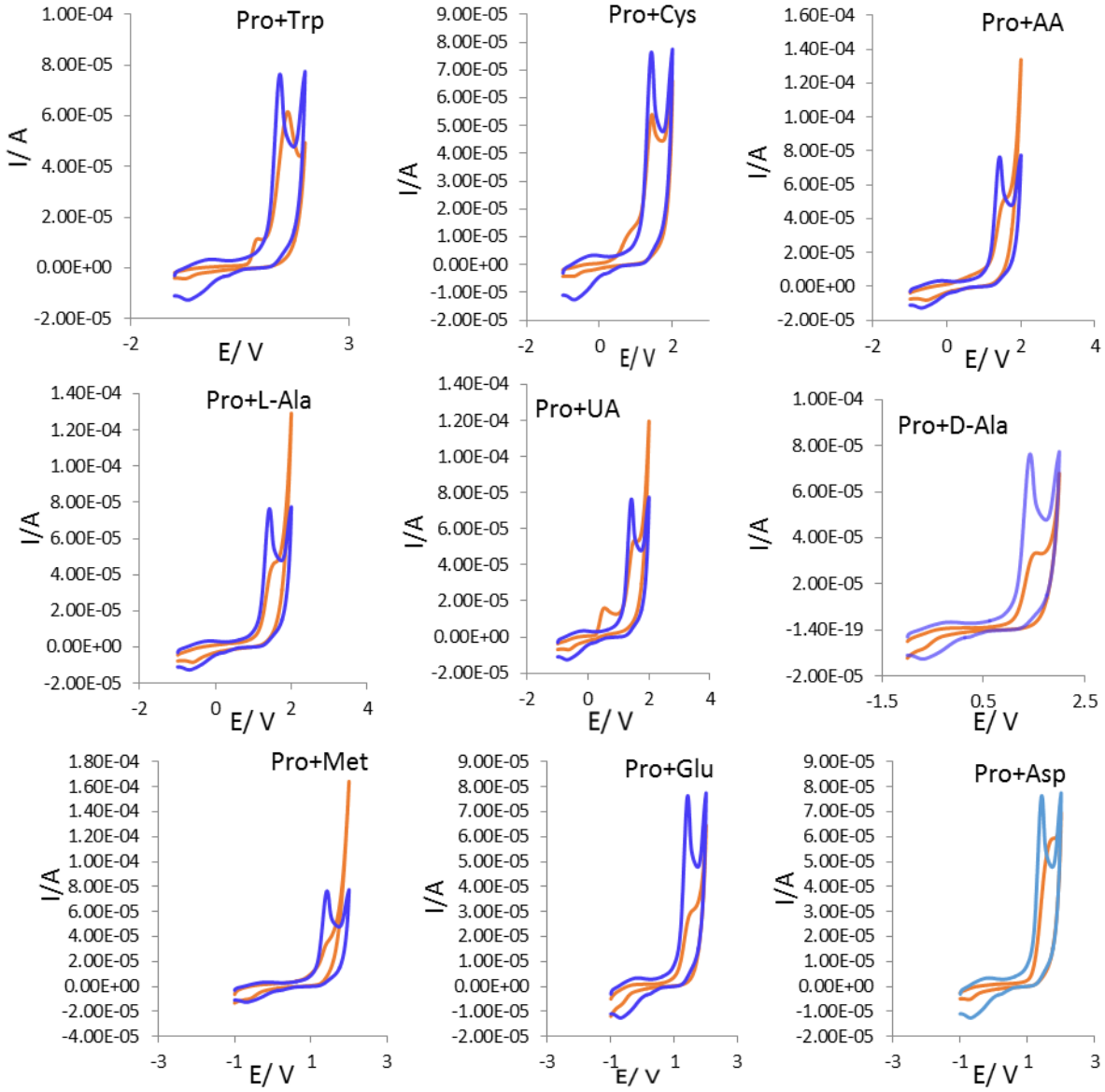

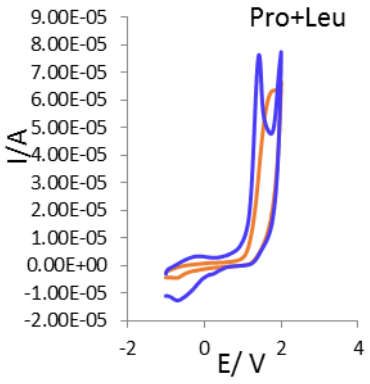

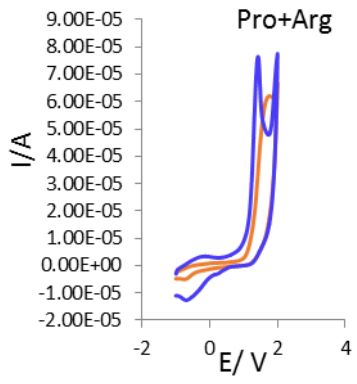

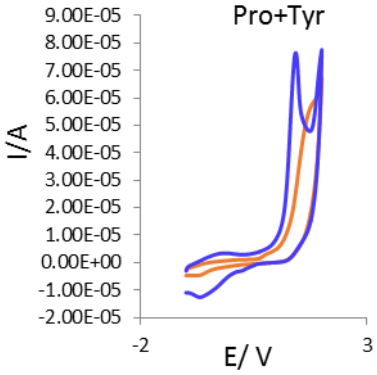

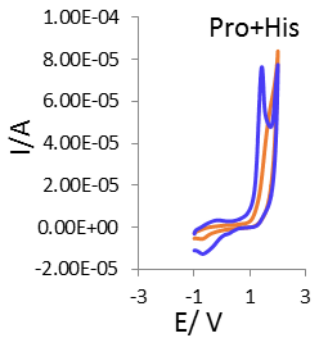

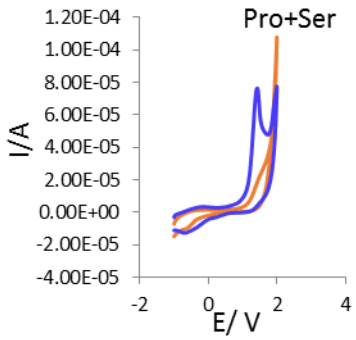

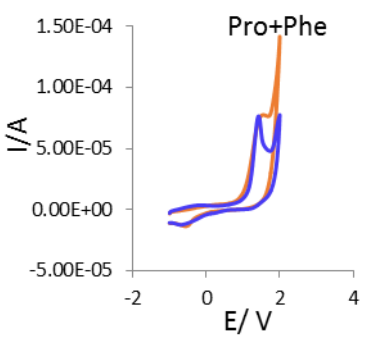

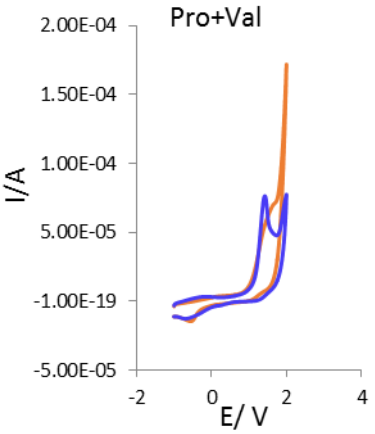

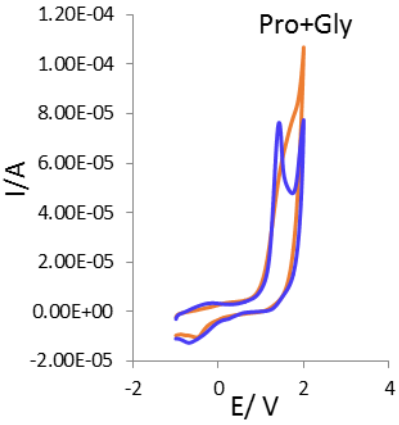

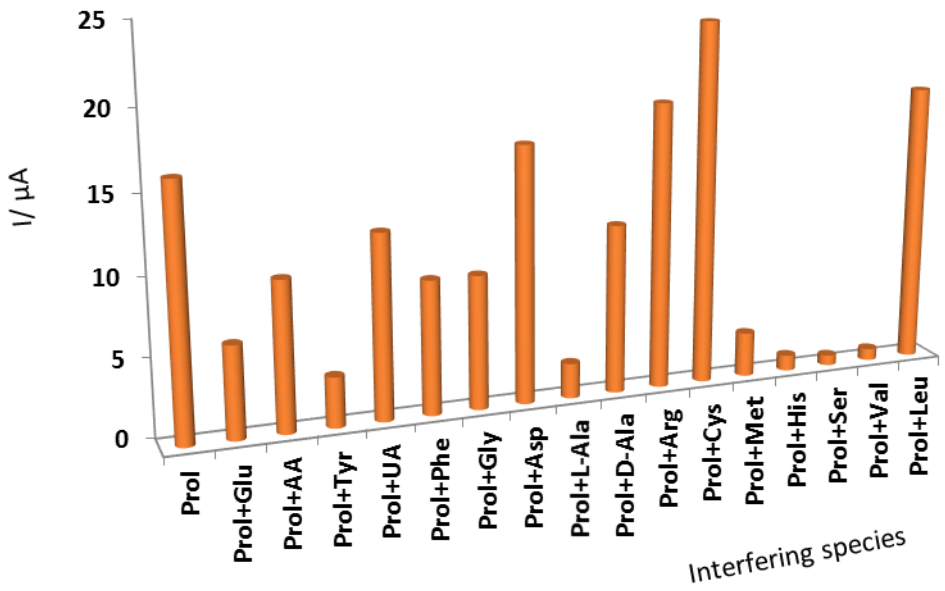

Fig. 5: CVs of PRODH-MMSNP-nPrNH$_2$-PCys-**CS**-GCE in the presence of different interfering species and its histogram. The concentration of L-Pro and interfering species were 0.004 g.ml $^{-1}$. Sweep rate is 100 mV.s^{-1}. Supporting electrolyte is 0.1M PBS, pH=7.4

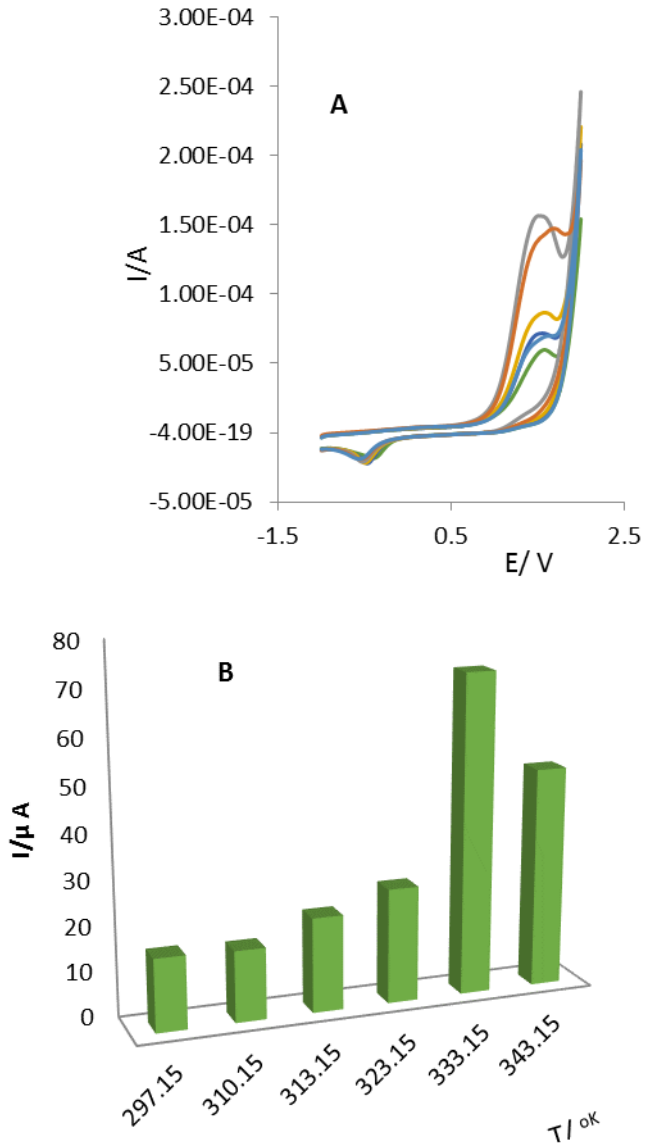

Fig. 6: **A)** CVs of PRODH-MMSNP-nPrNH$_2$-PCys-CS-GCE in different temperature of solution (297.15, 310.15, 313.15, 323.15, 333.15, and 343.15 ^{o}K). **B**) Dependency of peak current *versus* temperature of solution. The concentration of L-Pro was 0.004 g.ml $^{-1}$. Sweep rate is 100 mV.s^{-1}. Supporting electrolyte is 0.1M PBS, pH=7.4.

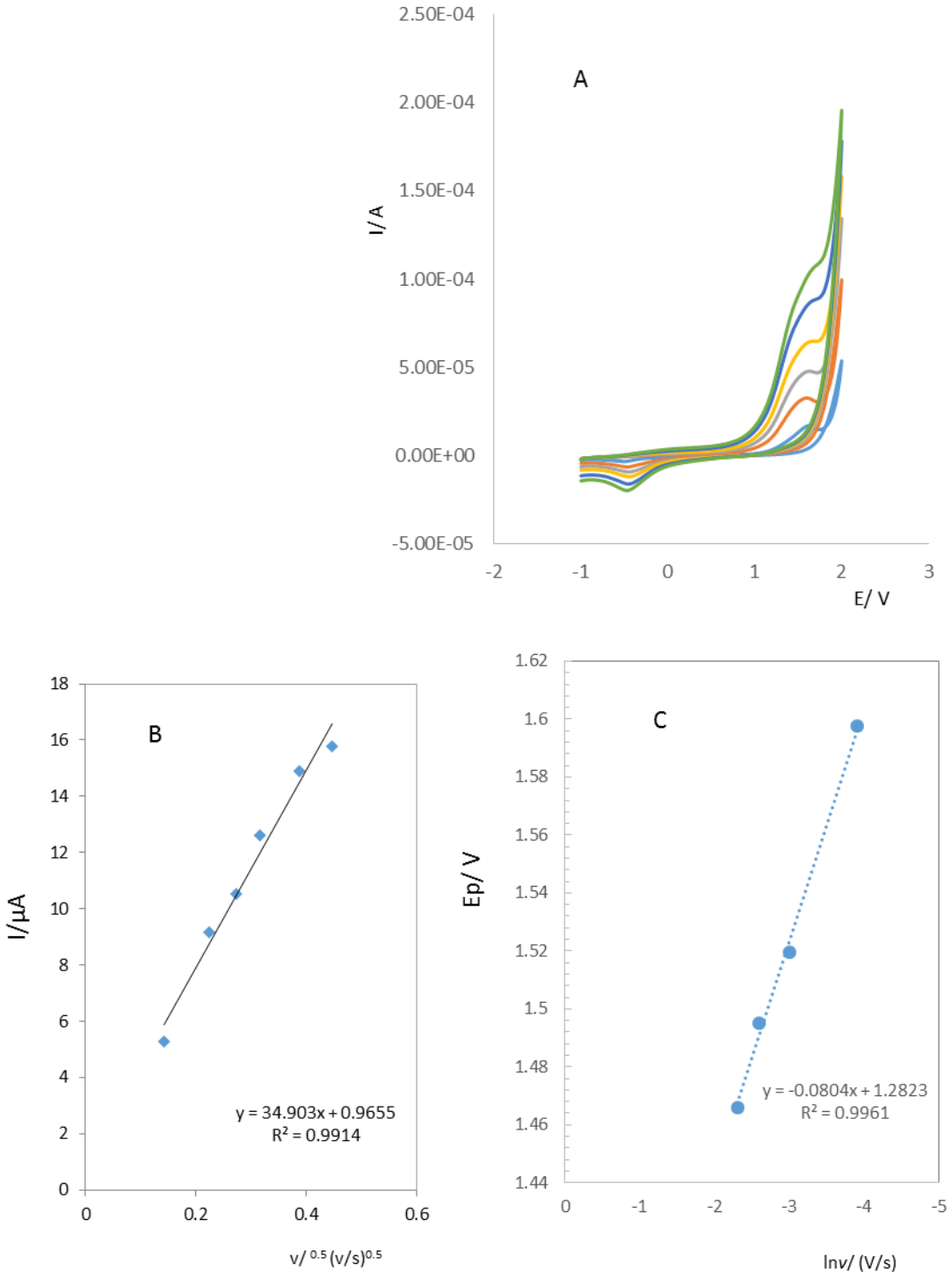

FIG. 7: A) CVs of a PRODH-MMSNP-nPrNH$_2$-PCys-CS-GCE in the presence of 0.004 g/ml of L-Pro+0.1M PBS, pH=7.4 in various potential sweep rates (20-200 mV/s). **B)** Dependency of oxidation peak currents *versus* square root of scan rate using CVs of PRODH-MMSNP-nPrNH$_2$-PCys-CS-GCE; **C**) The plot of oxidation peak potentials *versus* neperian logarithm of scan rates using PRODH-MMSNP-nPrNH$_2$-PCys-CS-GCE. The concentration of L-Pro was 0.004 g/ml . Supporting electrolyte is 0.1M PBS, pH=7.4.

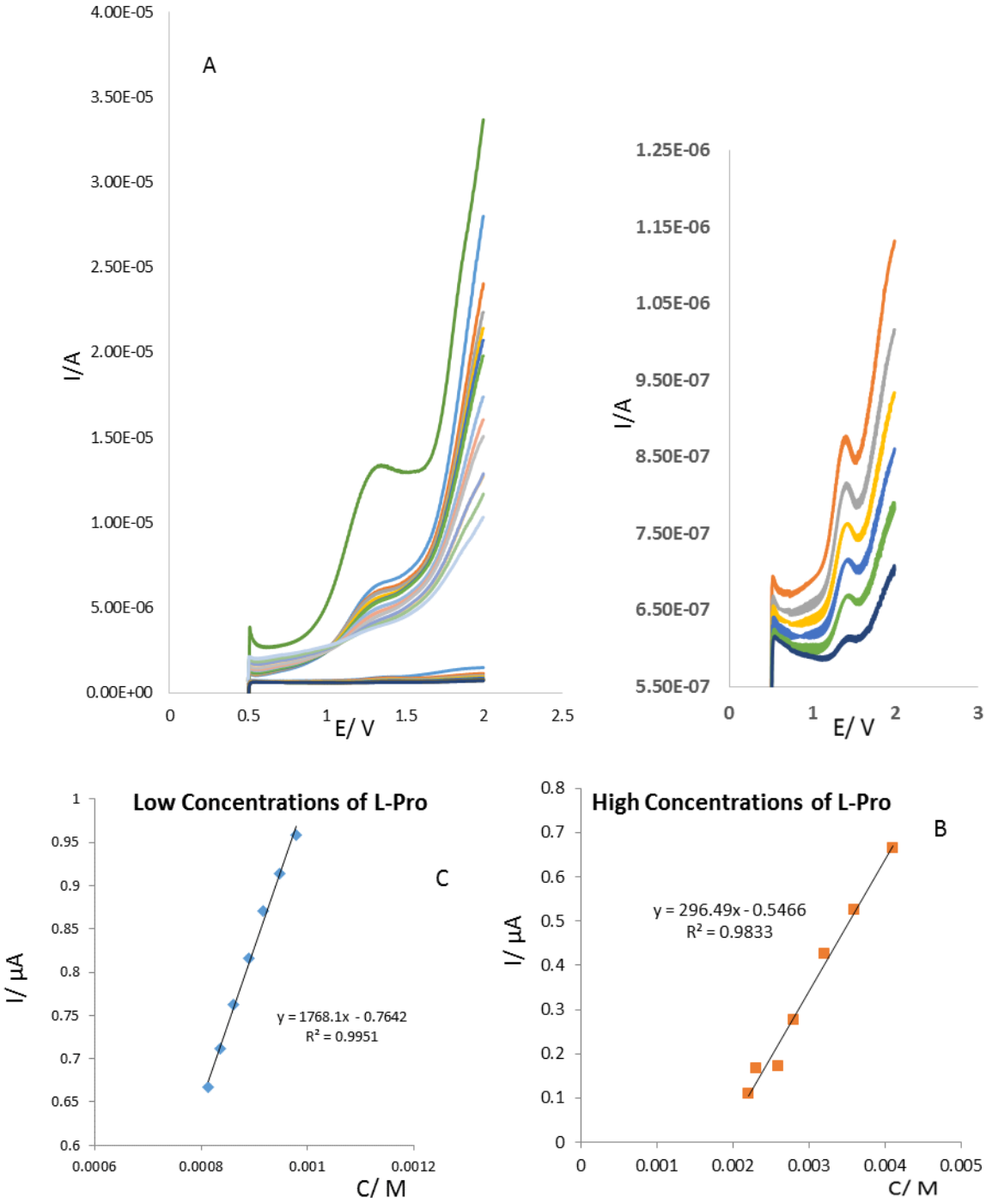

FIG. 8. A) DPVs obtained for determination of L-Pro in 0.1M PBS using PRODH-MMSNP-nPrNH_2-PCys-CS-GCE. L-Pro concentrations are as: 0.034, 0.015, 0.01, 0.007, 0.005, 0.0048, 0.0041, 0.0036, 0.0032, 0.0028, 0.0026, 0.0023, 0.0022, 0.002, 0.0019, 0.0017, 0.0016, 0.00158, 0.0015, 0.00142, 0.00136, 0.00129, 0.00124, 0.0011, 0.00114, 0.00109, 0.00105, 0.00101, 0.00098, 0.000949, 0.000918, 0.00089, 0.000862, 0.000837, 0.000813, 0.00079, 0.00076, 0.00074, 0.00072, and 0.00071 M. **Inset** is DPVs of L-Pro in low concentrations. (**B and C)** Calibration curve of L-Pro in high (**B**) and low (**C**) concentrations. Pulse amplitude: 0.05 V. Pulse width: 0.05 s. Pulse period: 0.2 s. Scan rate: 5 mVs^{-1}. (SD=3.1±.18, n=5)

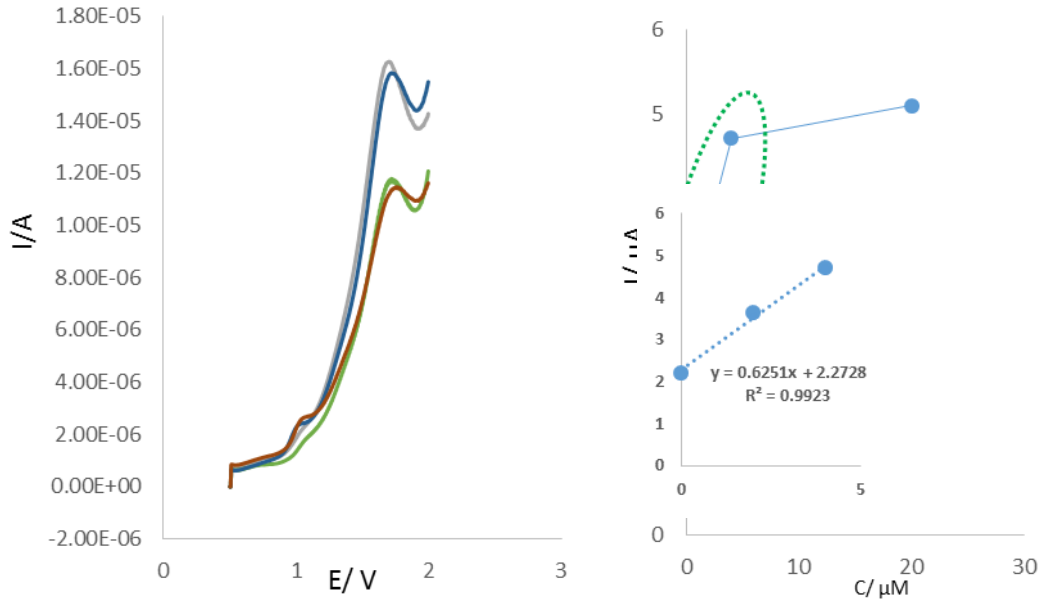

Fig. 9: DPVs of spiked whole blood samples in different concentration (0.001, 2, 4, and 20 µM) using PRODH-MMSNP-nPrNH$_2$-PCys-CS-GCE. Inset is concentration profile. Pulse amplitude: 0.05 V. Pulse width: 0.05 s. Pulse period: 0.2 s. Scan rate: 5 mVs^{-1}.

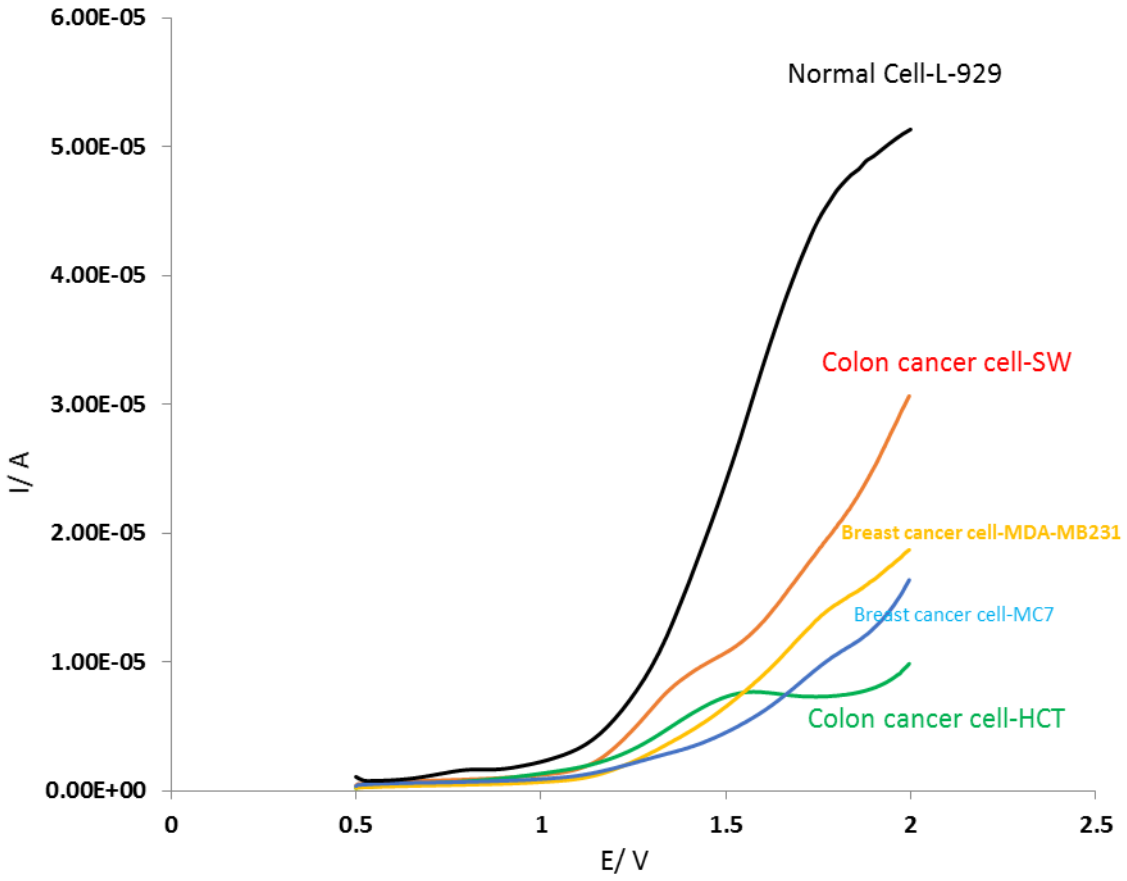

Fig. 10: SWVs of normal cell (L929) and different cancer cells such as gastric cancer cell-CAT 3, colon cancer cell-HCT, colon cancer cell-SW, and breast cancer cell-MCF7 using PRODH-MMSNP-nPrNH$_2$-PCys-CS-GCE. Pulse amplitude: 0.05 V. Pulse width: 0.05 s. Pulse period: 0.2 s. Scan rate: 5 mVs^{-1}.

Table 1: Electrochemical characterization of different electrodes

Type of Enzyme based sensor	Electrochemical parameters			
	E_{pa}/V	E_{pc}/V	I_{pa}/µA	I_{pc}/µA
PRODH-MMSNP-nPrNH$_2$-PCys-CS-GCE	1.412	1.30	46.9	-7.00
PRODH-MMSNP-nPrNH$_2$-PCys-GCE	1.399	-	32.9	-
PRODH-MMSNP-nPrNH$_2$-GCE	1.492	1.558	15.4	-2.34

Table 2: Tested whole blood samples

Sample Type	Added Concentration	Calculated Concentration	Recovered Concentration %
Whole Blood	50 mM	50.05 mM (SD=4.17, n=5)	100.10
	40 µM	40.86 µM (SD=4.22, n=5)	102.15
	1 µM	1.10 µM (SD=5.00, n=5)	110.00

Table 3. Electrochemical parameters of SWVs of normal and different cancer cells using PRODH-MMSNP-nPrNH$_2$-PCys-β-CD-GCE. (SD=3.56, n=3)

Type of Cells	Peak height/µA	Peak position/ V
Normal cell (L929)	5.94	1.7393
Breast cancer cell-MCF73	0.199	1.7589
Colon cancer cell-HCT	2.44	1.5172
Colon cancer cell-SW	0.94	1.3611
Breast cancer cell-MCF7	0.59	1.7589